Symmetry and Dynamics of a Magnetic Oscillator

Sang-Yoon KIM*

Department of Physics, Kangwon National University, Chunchon 200-701

(Received 26 September 1997)

We consider a permanent magnetic dipole in an oscillating magnetic field. This magnetic oscillator has two dynamical symmetries. The breakdown and the restoration of these symmetries are investigated by varying the amplitude A of the magnetic field. For small A, symmetric states exist with respect to one of the two symmetries. However, such symmetric states lose their symmetries via symmetry-breaking pitchfork bifurcations, and then the symmetry-broken states exhibit period-doubling transitions to chaos. Consequently, small chaotic attractors with broken symmetries appear. However, as A is further increased they merge into a large symmetric chaotic attractor via symmetry-restoring attractor-merging crisis.

We consider a magnetic oscillator consisting of a permanent magnetic dipole of moment m placed in a spatially uniform magnetic field B that oscillates periodically in time. Its motion can be described by a second-order nonautonomous ordinary differential equation [1–3]:

$$I\ddot{\theta} + b\dot{\theta} + mB_0 \cos\omega t \sin\theta = 0, \tag{1}$$

where the overdot denotes the differentiation with respect to time, θ is the angle between the magnetic dipole and the magnetic field, I is the moment of inertia of the magnetic dipole about a rotation axis, b is the damping parameter, and B_0 and ω are the amplitude and the frequency of the periodically oscillating magnetic field B, respectively. Making the normalization $\omega t \to 2\pi(t + \frac{1}{2})$ and $\theta \to 2\pi x$, we have

$$\ddot{x} + \Gamma\dot{x} - A\cos 2\pi t \sin 2\pi x = 0, \tag{2}$$

where x is a normalized angle with range $x \in [-\frac{1}{2}, \frac{1}{2})$, $\Gamma = 2\pi b/I\omega$, and $A = 2\pi m B_{ac}/I\omega^2$. Note also that this equation of motion is the same as that of a particle in a standing-wave field [4,5].

For the conservative case of $\Gamma = 0$, the Hamiltonian system exhibits period-doubling bifurcations and large-scale stochasticity, which have been found both experimentally [1–3] and numerically [4,5], as the normalized amplitude A is increased. Here we are interested in the dissipative case of $\Gamma \neq 0$. An experiment on period-doubling bifurcations in a dissipative system has been reported [2].

The normalized equation of motion (2) can be reduced to two first-order ordinary differential equations:

$$\dot{x} = y, \tag{3a}$$

$$\dot{y} = -\Gamma y + A\cos 2\pi t \sin 2\pi x. \tag{3b}$$

These equations have two symmetries, S_1 and S_2, because the transformations

$$S_1 : \quad x \to x \pm \frac{1}{2},\ y \to y,\ t \to t \pm \frac{1}{2}, \tag{4}$$

$$S_2 : \quad x \to -x,\ y \to -y,\ t \to t, \tag{5}$$

leave Eq. (3) invariant. The transformations in Eqs. (4) and (5) are just the shift in both x and t and the (space) inversion, respectively. Hereafter, we will call S_1 and S_2 the shift and the inversion symmetries, respectively. If an orbit $z(t)[\equiv (x(y), y(t))]$ is invariant under S_i $(i = 1, 2)$, it is called an S_i-symmetric orbit. Otherwise, it is called an S_i-asymmetric orbit and has its "conjugate" orbit $S_i z(t)$.

In this paper, by varying the amplitude A we study the evolutions of both the stationary states and the rotational states of period 1 in the magnetic oscillator for a moderately damped case of $\Gamma = 1.38$. Particularly, the breakdown and the restoration of the symmetries are investigated. As will be seen below, the dynamical symmetries are eventually broken through symmetry-breaking pitchfork bifurcations [6], which results in the birth of completely symmetry-broken states. These symmetry-broken states undergo period-doubling transitions to chaos [7], leading to the creation of small chaotic attractors with broken symmetries. However, as A is further increased they merge into a large symmetric chaotic attractor through a symmetry-restoring attractor-merging crisis [8].

The surface of section for the periodically-driven magnetic oscillator is the Poincaré time-1 map. Hence the Poincaré maps of an initial point z_0 $[= (x_0, y_0)]$ can be computed by sampling the orbit points z_m at the discrete time $t = m$ $(m = 1, 2, 3, \ldots)$. We call the transformation $z_m \to z_{m+1}$ the Poincaré map and write $z_{m+1} = P(z_m)$.

*E-mail: sykim@cc.kangwon.ac.kr

The linear stability of a q-periodic orbit of P such that $P^q(z_0) = z_0$ is determined from the linearized-map matrix $DP^q(z_0)$ of P^q at an orbit point z_0. Here P^q means the q-times iterated map. Using the Floquet theory [9], the matrix M ($\equiv DP^q$) can be obtained by integrating the linearized equations for the small displacements,

$$\delta\dot{x} = \delta y, \tag{6a}$$

$$\delta\dot{y} = -\Gamma\delta y + 2\pi A \cos 2\pi t \cos 2\pi x\, \delta x \tag{6b}$$

with two initial displacements $(\delta x, \delta y) = (1, 0)$ and $(0, 1)$ over the period q. The eigenvalues, λ_1 and λ_2, of M are called the Floquet (stability) multipliers, characterizing the orbit stability. After some algebra, we find that the determinant of M is given by $det(M) = e^{-\Gamma q}$. Hence the pair of Floquet multipliers of a periodic orbit lies either on the circle of radius $e^{-\Gamma q/2}$ or on the real axis in the complex plane. The periodic orbit is stable only when both Floquet multipliers lie inside the unit circle. Hence the periodic orbit can lose its stability only when a Floquet multiplier λ decreases (increases) through -1 (1) on the real axis. When a Floquet multiplier λ decreases through -1, the periodic orbit loses its stability via period-doubling bifurcation. On the other hand, when a Floquet multiplier λ increases through 1, it becomes unstable via pitchfork or saddle-node bifurcation. For more details on bifurcations, refer to Ref. 6.

We first consider the case of the stationary states. The magnetic oscillator has two stationary states $\hat{z}$. The first one is $\hat{z}_I = (0, 0)$ and the second one is $\hat{z}_{II} = (\frac{1}{2}, 0)$. These stationary states are symmetric with respect to the inversion symmetry S_2, while they are asymmetric and conjugate with respect to the shift symmetry S_1. Hence they are partially symmetric orbits with only the inversion symmetry S_2. We also note that the two stationary states are the fixed points of P [*i.e.*, $P(\hat{z}) = \hat{z}$ ($\hat{z} = \hat{z}_I, \hat{z}_{II}$)]. We investigate the evolution of the fixed points $\hat{z}_I$ and $\hat{z}_{II}$ with increasing A. For $A = 3.142\,710\cdots$, each fixed point loses its stability through a symmetry-conserving period-doubling bifurcation, leading to the birth of a new stable S_2-symmetric orbit with period 2. An example for $A = 3.31$ is shown in Fig. 1(a). Like the fixed points, the two stable period-doubled orbits with the inversion symmetry S_2, whose phase portraits are denoted by solid lines, are asymmetric and conjugate ones with respect to the shift symmetry S_1. The Poincaré map of the stable 2-periodic orbit encircling the unstable fixed point $\hat{z}_I$ [$\hat{z}_{II}$] is also represented by a solid circle (square). However, as A is further increased each of the two S_2-symmetric orbits of period 2 becomes unstable via S_2-symmetry-breaking pitchfork bifurcation for $A = A_{b,s}$ ($= 3.817\,897\cdots$). Consequently, two conjugate pairs of new S_2-symmetry-broken orbits with period 2 appear for $A > A_{b,s}$. An example for $A = 3.87$ is given in Fig. 1(b). One S_2-conjugate pair encircles the unstable fixed point $\hat{z}_I$, while the other pair encircles the unstable fixed point $\hat{z}_{II}$. For each S_2-conjugate pair, the phase portrait (Poincaré map) of one orbit is denoted by a solid line [solid symbol (circle or square)], whereas that of the other one is represented by a dashed line [open symbol (circle or square)]. Thus the two symmetries S_1 and S_2 are completely broken.

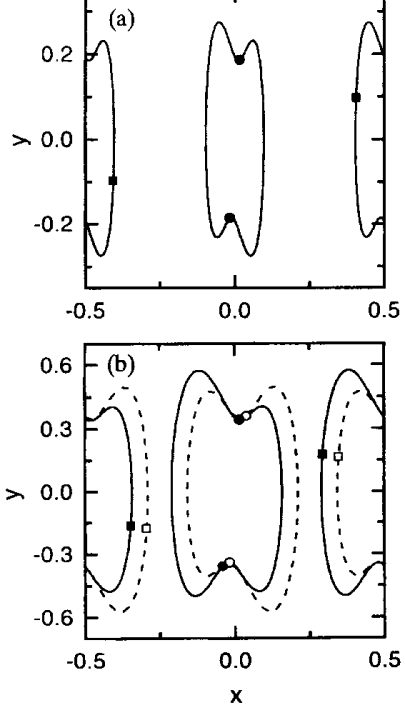

Fig. 1. Symmetry-conserving and symmetry-breaking bifurcations. Two stable period-doubled orbits with the inversion symmetry S_2 are born from the two fixed points via symmetry-conserving period-doubling bifurcations. They are shown in (a) for $A = 3.31$. Their phase portraits (Poincaré maps) are denoted by solid lines [solid symbols (circle and square)]. The two S_2-symmetric orbits with period 2 become unstable via S_2-symmetry-breaking pitchfork bifurcations. Consequently, two S_2-conjugate pairs of stable orbits with period 2 appear, as shown in (b) for $A = 3.87$. For each S_2-conjugate pair, the phase portrait (Poincaré map) of one orbit is denoted by a solid line [solid symbol (circle or square)], while that of the other one is represented by a dashed line [open symbol (circle or square)].

With increasing A, each of the four 2-periodic orbits with completely broken symmetries undergoes an infinite sequence of period-doubling bifurcations, ending at a finite critical point A_s^* ($= 3.934\,787\cdots$) as in the case of the one-dimensional maps [7]. For $A > A_s^*$, four small S_1- and S_2-asymmetric chaotic attractors with the largest positive Lyapunov exponent σ, characterizing the average exponential rate of divergence of nearby orbits [10], appear. As A is further increased, the different parts of each chaotic attractor coalesce and form larger pieces. Through such a band-merging process, each chaotic attractor eventually becomes composed of two pieces. An example for $A = 3.9411$ is given in Fig. 2(a).

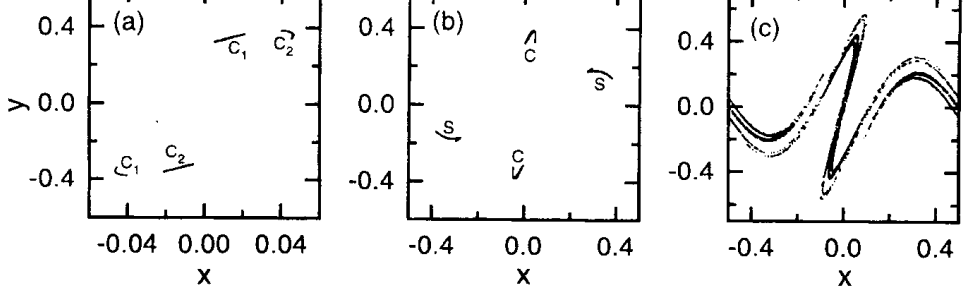

Fig. 2. Poincaré-map plots of chaotic attractors after the period-doubling transitions to chaos for the case of the fixed points. An S_2-conjugate pair of small chaotic attractors, c_1 and c_2, near the unstable fixed point $\hat{z}_I$ are shown in (a) for $A = 3.9411$. Each of them consists of two pieces. These two chaotic attractors merge into a bigger one c via S_2-symmetry-restoring crisis. For $A = 3.95$ the chaotic attractor c with the inversion symmetry S_2 and its S_1-conjugate one s are shown in (b). These two small chaotic attractors also merge into a larger one via S_1-symmetry-restoring crisis. A single large chaotic attractor with completely restored S_1 and S_2 symmetries is shown in (c) for $A = 3.975$.

For the sake of convenience, only the two chaotic attractors with $\sigma \simeq 0.189$, denoted by c_1 and c_2, near the unstable fixed point $\hat{z}_I$ are shown; in fact, their conjugate chaotic attractors with respect to the S_1 symmetry exist near the unstable fixed point $\hat{z}_{II}$. As A exceeds a 1st critical value $A_{c,1}$ (= 3.9484), the two chaotic attractors c_1 and c_2 merge into a bigger one c via S_2-symmetry restoring crisis. As an example, a chaotic attractor c with $\sigma \simeq 0.307$ is shown in Fig. 2(b) for $A = 3.95$, and its conjugate one with respect to the S_1 symmetry is denoted by s. These two chaotic attractors, c and s, become S_2-symmetric (but still S_1-asymmetric). Thus the inversion symmetry S_2 is restored first. However, as A passes through a 2nd critical value $A_{c,2}$ (= 3.9672) the two small chaotic attractors, c and s, also merge to form a larger one via S_1-symmetry-restoring crisis. An example for $A = 3.975$ is shown in Fig. 2(c). Note that the single large chaotic attractor with $\sigma \simeq 0.599$ is both S_1- and S_2-symmetric. Thus the two symmetries S_1 and S_2 are restored completely, one by one, via two successive symmetry-restoring crises.

We now study the evolution of the rotational states of period 1 with increasing A. A pair of stable and unstable rotational orbits with period 1 is born for $A \simeq 2.771$ through a saddle-node bifurcation. In contrast to the stationary states, the rotational states are S_1-symmetric, but S_2-asymmetric. As an example, a conjugate pair of S_2-asymmetric rotational states for $A = 3.31$ is shown in Fig. 3(a). The phase portrait (Poincaré map) of the orbit with positive angular velocity is denoted by a solid line (solid circle), while that of the other orbit with negative angular velocity is represented by a dashed line (open circle). With increasing A, each stable S_1-symmetric rotational orbit with period 1 loses its stability for $A = A_{b,r}$ (= 9.892 445 $\cdots$) via S_1-symmetry-breaking pitchfork bifurcation. Consequently, two conjugate pairs of S_1-symmetry-broken orbits with period 1 appear for $A > A_{b,r}$. An example for $A = 11.1$ is given in Fig. 3(b). The phase portrait (Poincaré map) of one S_1-conjugate

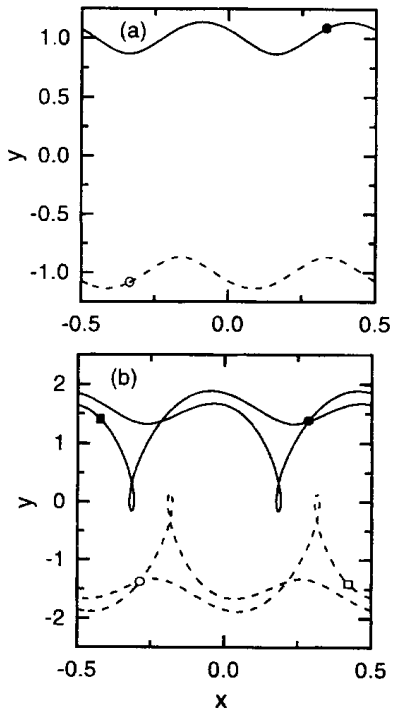

Fig. 3. Saddle-node and symmetry-breaking pitchfork bifurcations. A conjugate pair of the S_2-asymmetric rotational orbits with period 1 born via saddle-node bifurcations is shown in (a) for $A = 3.31$. These two orbits of period 1 are S_1-symmetric. The phase portrait (Poincaré map) of the orbit with positive angular velocity is denoted by a solid line (solid circle), whereas that of the other orbit with negative angular velocity is represented by a dashed line (open circle). The two S_1-symmetric orbits with period 1 lose their stability via S_1-symmetry-breaking pitchfork bifurcations. Consequently, two S_1-conjugate pairs of stable orbits with period 1 appear, as shown in (b) for $A = 11.1$. The phase portrait (Poincaré map) of one S_1-conjugate pair is denoted by a solid line [solid symbols (circle and square)], whereas that of the other pair is represented by a dashed line [open symbols (circle and square)].

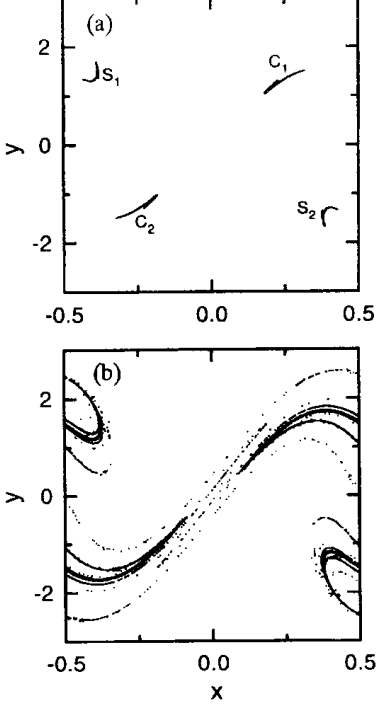

Fig. 4. Poincaré-map plots of chaotic attractors after the period-doubling transitions to chaos for the case of the rotational orbits with period 1. Four small chaotic attractors, denoted by c_1, c_2, s_1, and s_2, are shown in (a) for $A = 12.342$. These four small chaotic attractors merge into a larger one via a symmetry-restoring crisis. A single large chaotic attractor with simultaneously restored S_1 and S_2 symmetries is shown in (b) for $A = 12.4$.

pair with positive average angular velocity is denoted by a solid line [solid symbols (circle and square)], while that of the other pair with negative average angular velocity is represented by a dashed line [open symbols (circle and square)]. Thus the two symmetries S_1 and S_2 are completely broken.

With further increase of A, each of the four 1-periodic rotational orbits with completely broken symmetries exhibits an infinite sequence of period-doubling bifurcations, accumulating at a finite critical point A_r^* ($= 12.252\,903\cdots$), as in the case of the stationary states. For $A > A_r^*$, four small chaotic attractors appear. Through a band-merging process, the different parts of a chaotic attractor merge into larger pieces. Thus each chaotic attractor eventually consists of a single piece, as illustrated in Fig. 4(a) for $A = 12.342$. Four small chaotic attractors with $\sigma \simeq 0.416$ are denoted by c_1, c_2, s_1, and s_2, respectively. However, as A passes through a critical value A_c ($= 12.3424$), the four small chaotic attractors merge to form a larger one via symmetry-restoring crisis. An example for $A = 12.4$ is given in Fig. 4(b). We note that the single large chaotic attractor with $\sigma \simeq 0.713$ has both S_1 and S_2 symmetries. Thus the two symmetries S_1 and S_2 are restored simultaneously through one symmetry-restoring crisis, which is in contrast to the case of the stationary states.

In addition to the breakdown and the restoration of the symmetries discussed, the magnetic oscillator exhibits other interesting dynamical behaviors, such as period-doubling transitions to chaos, disappearance of large symmetric chaotic attractors via attractor-destroying crises or intermittencies, creation of new periodic attractors through saddle-node bifurcations, and a cascade of "resurrections" of the fixed points (*i.e.*, an infinite sequence of restabilizations and destabilizations of the fixed points). A detailed account of such rich dynamical behaviors will be given elsewhere [11].

ACKNOWLEDGMENTS

This work was supported by the Basic Science Research Institute Program, Ministry of Education, Project No. BSRI-97-2401.

REFERENCES

[1] V. Croquette and C. Poitou, J. Phys. Lett. **42**, 537 (1981).

[2] H. Meissner and G. Schmidt, Am. J. Phys. **54**, 800 (1986).

[3] K. Briggs, Am. J. Phys. **55**, 1083 (1987).

[4] J. Bialek, G. Schmidt and B. H. Wang, Physica **D14**, 265 (1985).

[5] G. Schmidt, Comments Plasma Phys. Controlled Fusion **7**, 87 (1982).

[6] J. Guckenheimer and P. Holmes, *Nonlinear Oscillations, Dynamical Systems, and Bifurcations of Vector Fields* (Springer-Verlag, New York, 1983), Sec. 3.5.

[7] M. J. Feigenbaum, J. Stat. Phys. **19**, 25 (1978); **21**, 669 (1979).

[8] For attractor-merging crises, refer to the following references: C. Grebogi, E. Ott, F. Romeiras and J. A. Yorke, Phys. Rev. **A36**, 5365 (1987); Y. Gu, M. Tung, J.-M. Yuan, D. H. Feng and L. Narducci, Phys. Rev. Lett. **52**, 701 (1984); V. Mehra and R. Ramaswamy, Phys. Rev. **E53**, 3420 (1996).

[9] J. Guckenheimer and P. Holmes, *Nonlinear Oscillations, Dynamical Systems, and Bifurcations of Vector Fields* (Springer-Verlag, New York, 1983), p. 24.

[10] A. J. Lichtenberg and M. A. Lieberman, *Regular and Chaotic Dynamics* (Springer-Verlag, New York, 1983), p. 262.

[11] S.-Y. Kim (unpublished).